33RD CONGRESS
OF THE INTERNATIONAL COUNCIL
OF THE AERONAUTICAL SCIENCES
STOCKHOLM, SWEDEN, 4-9 SEPTEMBER, 2022

ICAS 2022 SWEDEN

FATIGUE LIFE ENHANCEMENT OF TYPICAL AERONAUTICAL JOINTS BY MEANS OF ENGINEERED RESIDUAL STRESSES

D. Fanteria[1], L. Boni [1], F. Bovecchi [1], D. O. Busse[2] & D. Furfari[2]

[1]University of Pisa - Department of Civil and Industrial Engineering – Aerospace Section
Via G. Caruso, 8 – 56126 Pisa – Italy; e-mail: daniele.fanteria@unipi.it
[2]AIRBUS Operations GmbH, ZAL Tech Center,
Hein-Saß-Weg 22, 21129 Hamburg, Germany; e-mail: david-osman.busse@airbus.com

Abstract

The fatigue behaviour of a typical joint configuration, available in two variants, has been investigated, assessing also the influence of various life enhancement treatments. Different batches of specimens were evaluated: basic material, Tartaric Sulphuric Acid anodized and also coupons subjected to fatigue enhancement processes, such as Cold eXpansion and Laser Shock Peening. A numerical activity was also performed in order to assess the stress distribution in the specimens.

Keywords: fatigue, fastened joints, residual stresses, split sleeve cold expansion, laser shock peening

1. Introduction

The design of joints is really a challenge for aircraft fatigue specialists because most fatigue cracks in service originate from joints. Understanding the behavior of joints and its stress distribution is an obvious prerequisite for a correct dimensioning, so to guarantee a long safe life. The famous textbook by Prof. Schijve [1] includes a chapter dedicated to joints, where the main findings are shortly presented and discussed, in order to give to the student a view of the main difficulties in predicting the fatigue behavior of a joint. In the literature, AGARD programs [2-3] have been a milestone, pointing out the role of typical parameters that influence deeply the stress distribution, such as load transfer and secondary bending (both depend strictly on the joint geometry), plus the role of technological/installation parameters, such as the type of hole, the type of fastener and the installation fit. Two large experimental programs were coordinated and included the participation of various laboratories, in different NATO countries, where tests were performed on a number of different specimen geometries; the analysis of the results allowed to point out how the various parameters could influence the fatigue performance of the joint. A few years later, an important contribution came from Jarfall [4], who presented the analysis methodology used in Saab-Scania for evaluating the joint performances. Another group of Swedish authors [5] about ten years later performed a research program on the fatigue behavior of a few groups of joints, that differed for the fastener type and installation methodology: an evaluation of the technological aspects was so performed, on the basis of the comparison of the results.

The theoretical basis of the approach proposed by classical authors [1, 4] relies on the application of the superposition principle for the calculation of the highest punctual stress in the joint (or the stress concentration factor, if referred to a reference stress level). The superposition principle considers, in a simplified manner, the stress in the critical point of the joint as the sum of three contributions:

(a) The stress due to the load transferred, which can be evaluated considering the situation of a pin-loaded hole.
(b) The stress due to the by-pass load, complementary to the previous contribution, which can be assessed considering the situation of a filled hole in tensile loaded plate.
(c) The additional stress component due to the presence of secondary bending (SB), which is more delicate to be estimated since the relationship between applied load and SB is non-linear.

Additional features of the joint, relevant to the technology (type of fastener, tool for hole drilling, installation fit, tightening couple), are normally kept into consideration by means of empirical coefficients, based on the relative position of S-N curves referred to the various situations. Each industrial manufacturer normally uses its own data basis and fitting parameters.

Notwithstanding decades of research on the subject and numerous analytical and numerical methods developed over the years, ad hoc experimental campaigns remain the only viable option [5] for assessing the fatigue properties of mechanically fastened joints. Consequently, a study has been started at the University of Pisa on the fatigue behavior of a particular class of joints commonly used in aircraft fuselage structures: the so-called “stringer coupling”. Such joint is used when two fuselage sections must be connected during the final assembly of the aircraft and so each longitudinal stringer is butt-jointed across the fuselage sections. In fuselage structures, the stringer geometry changes along the peripheral circumference – because of different load intensities – therefore, different stringer sections are used.

For this activity, simple specimens have been designed and they are composed by three elements of different materials, thickness, and form, connected by four titanium fasteners. Two different types of specimens have been defined by adopting two sets of thicknesses of the connected elements, while the other dimensions (width, length, hole diameters and spacing) remained the same for both variants. For each variant, four different groups of specimens have been prepared: basic (no specific treatment, to obtain reference results), anodized (by means of a Tartaric Sulphuric Anodization process), anodization plus split sleeve Cold eXpansion (CX) and anodization plus Laser Shock Peening (LSP). The research is a collaborative effort with Airbus Operations GmbH that contributed to the manufacturing of the specimens by providing the material and applying the TSA and the LSP treatments.

The paper presents the results of the experimental activity for the two specimen variants, pointing out the differences in Constant Amplitude (CA) fatigue behavior. The effectiveness of engineered residual stresses, induced by CX and LSP treatments, in enhancing the fatigue life is discussed.

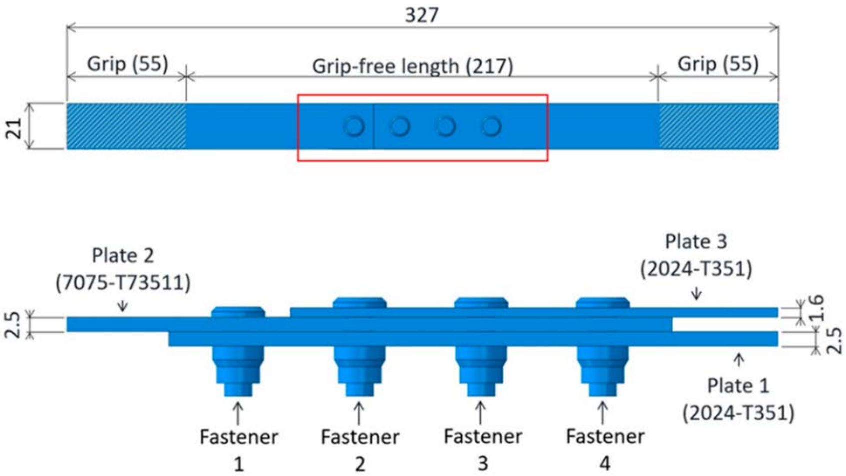

a) thin specimen

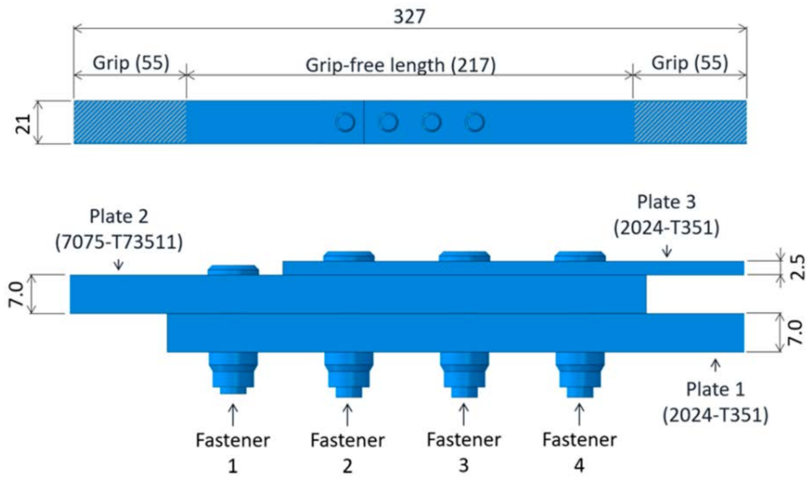

b) thick specimen

Figure 1 – Geometry of the two specimen variants.

2. Materials and methods

2.1 Design and validation of the joints test specimens

In fuselage structures, the stringer geometry changes along the peripheral circumference – because different load intensities occur – therefore, different stringer sections are defined. For this activity, a typical joint architecture has been selected, clearly inspired to transport aircraft drawings, and retaining the more significant characteristics albeit no reference to specific locations is implied.

Such architecture has been translated into two different types of specimens by adopting two sets of thicknesses of the connected elements: 2.5/2.5/1.6 mm for the thin variant and 7.0/7.0/2.5 mm for the thick one (see Figure 1).

The elements of the joints are made of AA alloys typically used in fuselage structures, namely: AA 2024-T351 has been used for plate like elements, while the stringer is represented in a simplified plate-like geometry, but it is made of extruded AA 7075-T73511 (indicated as plate 2 in figure 1). The fasteners are Hi-Tigue type EN6115K3 made of titanium alloy.

The two variants are indeed two different specimens because the fundamental parameters that influence the fatigue behavior of a joint are different: load transfer and secondary bending. Instead, the technological parameters, relative to hole preparation and fastener installation, remain the same for both variants. Also, the fastener diameter remains unaltered, while the shank length obviously changes to accommodate the elements to be joined; consequently, the stack-up over diameter ratio changes accordingly.

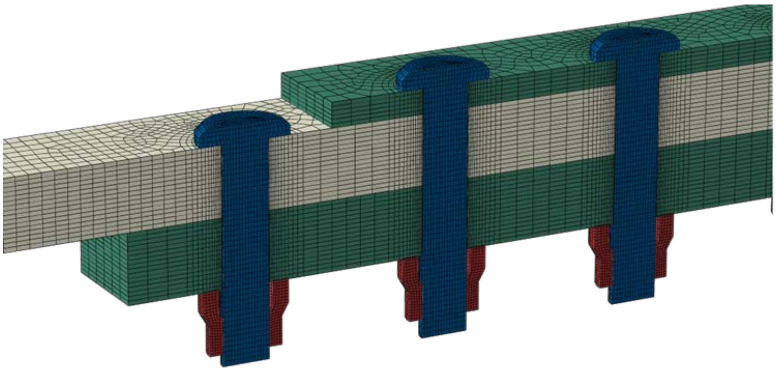

Figure 2 – Mesh example for the thick specimen FE model.

The design of the specimens was supported by numerical analysis, performed in SIMULIA ABAQUS, to study the stress distribution and the secondary bending effects of the stress in the hot spots. An example of a mesh of the model of the thick specimen variant is shown in Figure 2: solid elements have been used with grid spacing capable of capturing the stress distribution with a reasonable accuracy. An example of the results, in terms of principal stresses contour plots, is shown in figure 3.

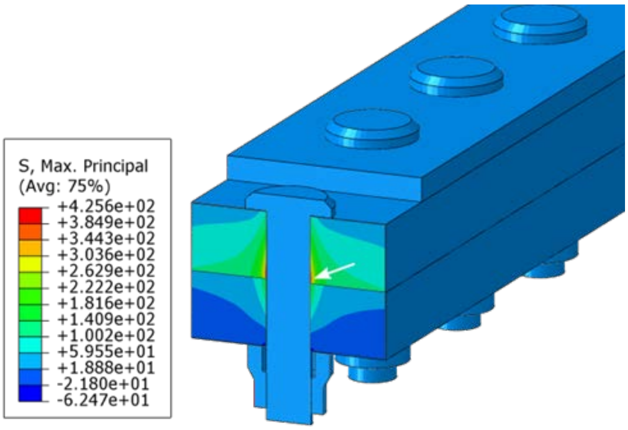

Figure 3 – Contour plot of max principal stress for the thick specimen FE analysis.

Table 1 presents FE results for stress ratios at critical locations in the thick specimen for a representative applied stress level. Results pertain to two analyses carried out considering different interference fits for the fasteners and show that for higher interferences, holes 1 and 4 can reach comparable stress ratios; this may induce crack initiation in both holes with comparable probabilities.

	Hole 1			Hole 2			Hole 3			Hole 4		
Analysis	**P1**	**P2**	**P3**	**P1**	**P2**	**P3**	**P1**	**P2**	**P3**	**P1**	**P2**	**P3**
Elasto-plastic No fit	3.2	6.0		2.7	3.6	2.7	2.9	2.6	2.9	4.5	2.6	4.4
Elasto-plastic Max fit	1.4	1.7		1.4	1.6	1.2	1.6	1.4	1.6	1.6	1.3	1.7

Table 1 – FE results for stress ratios at critical locations in the thick specimen.

In order to have a better view of the stress distribution in the two variants and, therefore, to better interpret the fatigue results, static tests have been performed on coupons instrumented with strain gauges, measuring also the out-of-plane joint displacements in selected reference locations. Photographs of the instrumented thick specimen ready for testing are shown in figure 4.

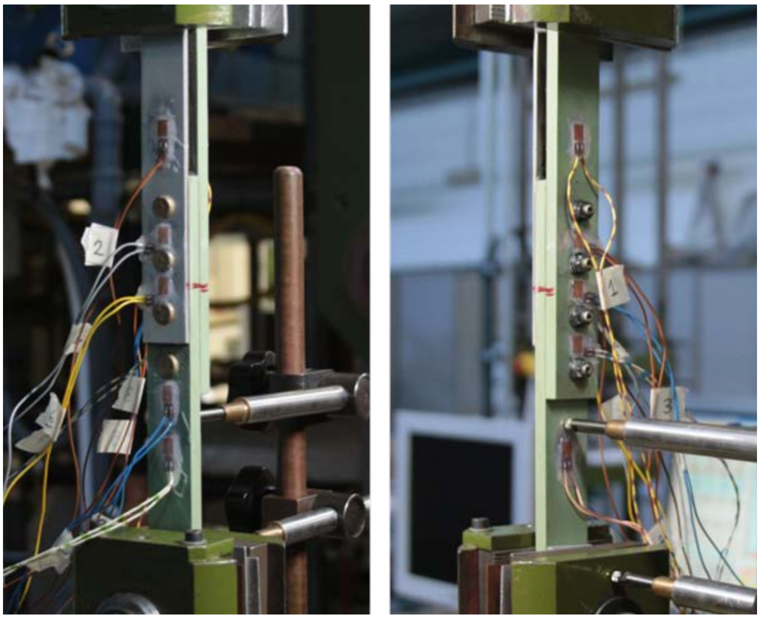

Figure 4 – Thick coupon instrumented with strain gauges.

A total of 10 Strain Gauges (SG), with 1.5 mm grid, have been bonded to the specimens in the locations indicated in figure 5. Whenever possible, SG have been installed in back-to-back configuration, so that bending strains in the instrumented section could be appreciated.

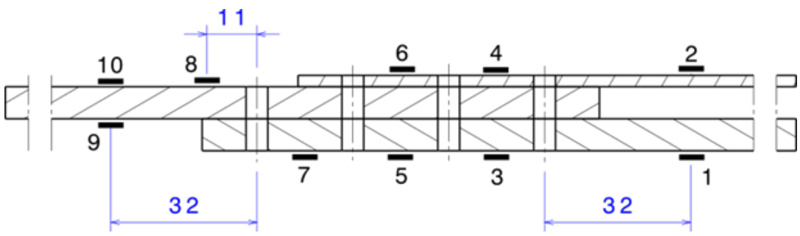

Figure 5 – Strain gauges numbering and positions.

As an example, a comparison of the strain distribution in the two configurations for the same applied reference stress, was carried out to evaluate differences in terms of the secondary bending measured in the neighborhood of the critical section by strain gauges 9 and 10 (Figure 5). According to the traditional definition of bending component expressed as a percentage of the membrane component, the two configurations show indeed different values: 9.6% for the thin joint and 31.2% for the thick one. The SB is a function of the applied load, in the sense that, under the action of a higher load, an eccentric joint tends to align the various centers of gravities of the different sections, stretching the specimen axially, and reducing the bending component with respect to the membrane component.

The results of the strain survey have been compared with those obtained from Finite Element models, for assessing the stress distribution, keeping also geometrical and constitutive non-linearity into account; an example of such comparison is given in table 2. A substantial agreement between numerically evaluated and measured strains can be observed.

SG n.	Exp.	FEM
1	635	787
2	2,160	1,948
3	565	552
4	974	1,031
5	413	390
6	627	704
7	155	63
8	618	972
9	2,295	2,205
10	1,175	1,372

Table 2 – Example of SG measurements (μm/m) compared to FE results for a given applied load.

2.2 Treatments of the specimen parts and specimen preparation

Material has been procured by Airbus DE who was responsible for the basic manufacturing of the parts that compose the joints (shaping and thickness reduction) and for the surface corrosion protection treatment that has been applied to all the specimens with exception of the basic specimen groups (in this case fabricated in bare aluminum alloy). The corrosion protection treatment selected was the Tartaric Sulfuric Anodization that was applied following Airbus industrial procedures typically employed on aircraft parts.

Hole drilling and fastener installation have been performed in Pisa following Airbus DE recommendations. To make the joint work in more realistic conditions, aircraft grade sealant (MC630, supplied by Airbus DE) was applied during fasteners installation.

The insertion of the fastener into the hole was performed by means of a special tool that was constructed for this purpose and connected to the piston of a 100 KN actuator: by commanding the piston movement in displacement control, it was possible to force the fastener stem into the hole in a controlled and repetitive way. Indeed, the light interference installation (0-30 μm) required axial forces of the order of 1500-1800 N, that could not be applied easily in different manners with the required characteristics of control.

2.3 Fatigue testing

The tests were performed under Constant Amplitude loading, characterized by a stress ratio equal to 0.1; a servo-hydraulic actuator of the capacity of 100 kN was used, for all the tests. The focus of the activity is to derive the Whöler curves for the joints in a range of lives comprised between 40 and 150 Kcycles. The load application frequency was in the range 2,5-4 Hertz.

The specimens were introduced in the grips using specific sets of shimmies, in order to align the centroid of the joint central section, namely the one made of three plates, to the loading actuator axis. Some secondary bending is present, which is different for the two variants, because of the difference in the load path eccentricity. The reference stress is simply the one applied to the central extruded element and the maximum force applied by the actuator was the product of the element cross section multiplied by the maximum cyclic stress.

2.4 Post processing of data and analysis of fracture surfaces

The fatigue tests results have been organized in S-N plots, and interpolated by means of traditional best-fit techniques, based on the least squares approach. In particular, a specific program has been used, based on the maximum likelihood criterion for considering also the run-outs. Further details can be found in [6].

The failure surfaces have been examined by means of optical and SEM fractographic analyses to identify potential anomalies such as multiple initiation points that could alter the results in a significant way. Such analysis proven useful since, in a few cases, allowed to identify causes for anomalous behavior (too short or excessively long lives for a given stress level) so that the results could be excluded from the Whöler curve fitting procedure.

3. Engineered residual stresses

3.1 Split sleeve Cold Expansion

The Cold eXpansion process was applied in Pisa, using Fatigue Technology Inc. (FTI) tools, and following the split sleeve protocol typically applied by Airbus DE. The starting hole was 4.32 mm in diameter, and the tool used was 4-4-N, which induces a maximum hole expansion of 4.7%. The holes were then reamed to the final 4.78 mm diameter. The expansion was applied at the same time to all the plates at a given hole, i.e. the whole stack-up was expanded contemporarily (see figure 6). The sleeve was introduced in such a way that the split was oriented along the load direction and the mandrel was introduced from the collar side, and it exited from the fastener head side. Fig. 6 shows a picture of the CX process application. In each Cx specimen, all the four holes were expanded, while in LSP specimens the Cx process was applied to holes 3 and 4 to avoid potential premature cracking (while holes 1 and 2 were LSP treated).

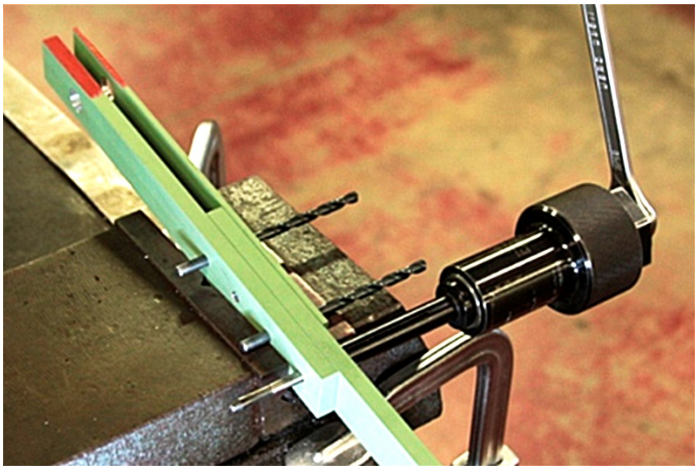

Figure 6 – Example of a thick specimen cold expansion.

	t [mm]	Power Density [GW/cm²]	Spot Diameter [mm]	X Overlap rate [%]	Y Overlap rate [%]	Offset rate [%]	Number of Layers	Overlay
Thick	7	2.5	3.5	25	25	25	4	Tape
Thin 1	2	0.7	-	50	50	-	4	Tape (steel)
Thin 2	2	0.7	-	86	86	-	1	none

Table 3: LSP parameters.

3.2 LSP treatment and residuals stress measurement

Laser peening of the stringer coupling samples was performed at the Center of Applied Aeronautical Research (ZAL TechCenter) in Hamburg using the Procudo200 LSP system. The Procudo LSP system set-up consists of a laser with a maximum energy capability of 10 J. The laser emits laser light with a wavelength of 1053 nm and operated for this work at a pulse frequency of 20 Hertz. The samples were manipulated through the stationary laser beam by Kuka industrial robots. As far as the confining medium is concerned, de-crystallized water was delivered to the surface of the workpiece by a water jet.

A photo of the Laser treatment facility is shown in figure 7.

Figure 7 – Procudo LSP system set-up.

Parameters for LSP treatments of the parts used to build the joint specimens are given in table 3.

4. Results and discussion

4.1 Residual stresses due to LSP

The LSP process parameters are numerous and influence the final result, i.e. the residual stress (RS) distribution, in a complex and interactive manner. A number of experimental attempts have been performed, followed by a measurement of RS in-depth distribution, typically by means of the hole drilling technique. For example, figure 8 shows the RS distribution on a 7 mm plate subjected to LSP on both sides. It can be seen that the residual compression is still high, also at the depth of about 1 mm, but not extremely high on the surface, where presumably crack initiation will take place. Therefore, a different shape of the residual compression can be considered as more appealing, as the two shown in figure 9, with a very high compression on the surface, that vanishes rapidly in depth. The best/optimum RS distribution may well be a function of the stress field applied in service by the external loads acting on the component under examination. The optimization is therefore a complex problem, that still requires time and experience.

4.2 Fatigue tests results

As already mentioned before, constant amplitude fatigue tests have been carried out, with a stress ratio equal to 0.1, in order to evaluate the fatigue behavior of the different specimen variants and in particular to appreciate the effects of the various processes applied to increase the joint life.

The two joints are geometrically similar and, apparently, differ only for the thickness of the components. In both cases, the reference stress is the one acting on the central element, the one made of the extrusion and representing the stringer. The change in thicknesses has two fundamental consequences that significantly influence the fatigue behavior of the element: the load transfer and the secondary bending in the critical fastener section. Therefore, the fatigue behavior of the two configurations is different and must be analyzed and presented separately.

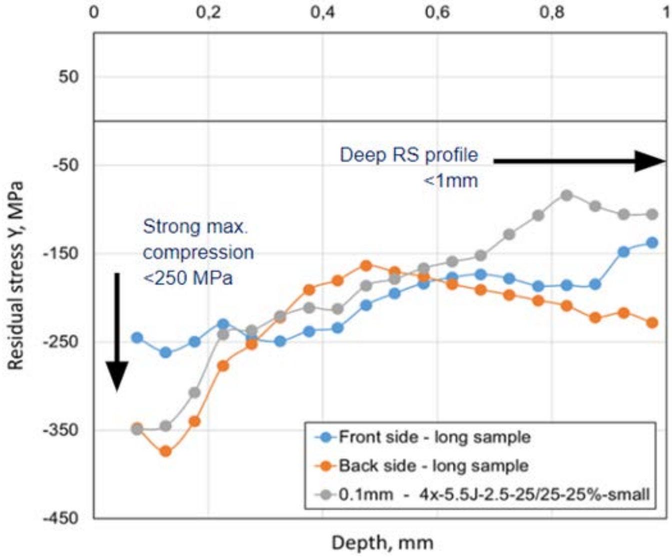

Figure 8 – Example of residual stress results on thick specimens.

The bare material specimens were tested first, not only because they were available before the others, but also in order to obtain a reference curve.

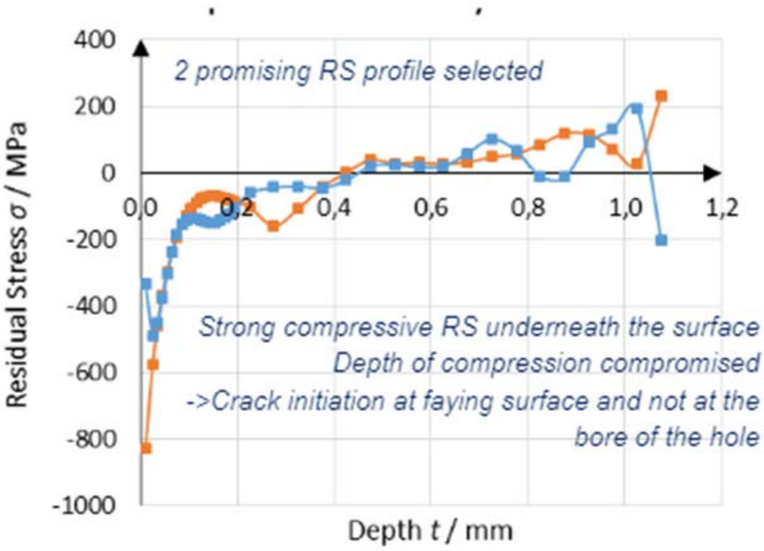

Figure 9 – Optimal residual stress profile for thick specimens.

4.2.1 Thick specimens

In this paragraph, the results of the thick specimens are presented, starting from those coming from the "basic" group of specimens, which were the first to be tested. In this group of results, it is important to observe that the failure modes associated with the tests performed at a low stress intensity is different from the one typical of the high stress levels. Fig. 10 shows, with filled data points, the results of the specimens in which a failure was also present at fastener number 4, i.e. the opposite to the one where failure was expected (and really initiated only there in the remaining samples). Once that failure initiated in a second dangerous location, the stress distribution changed and, when failure took place in that location, the remaining life of the joint was very short.

The observation of the fatigue failure area in the fracture surfaces can allow to understand where the crack initiated before; a larger fatigue area (in percentage to the total area) should mean that the nucleation started there. Apparently, there is a wide fatigue area at location 4, while close to hole 1 only a small fatigue area is present.

Moreover, secondary bending is a function of the applied load; so, these results may suggest that at higher stress levels hole 4 location remains critical, while at lower levels there is an almost equivalence between the two potential locations (holes 4 and 1).

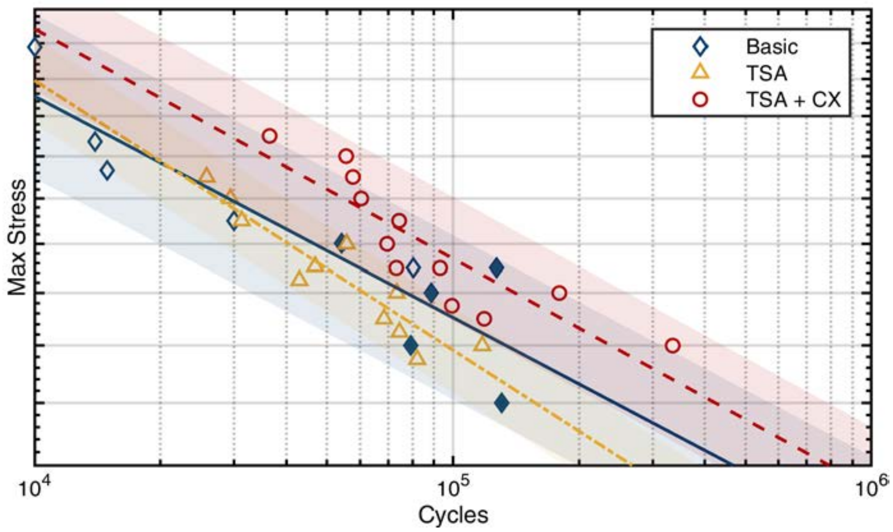

Fig. 10 – Whöler curves for thick variant: basic treatments

Though necessary for protection against corrosion, the application of an anodizing treatment induces a surface damage, that can be assimilated to a series of pits, that causes a reduction in the time-to-initiation of a fatigue crack. The problem is that the initiation normally takes place on the material surface, exactly where the negative influence of the anodizing treatment is explicated; the influence can be of course function of the stress distribution around the "hot spot" of the structure. For the assessment of the influence of this process on the joints considered in this activity, the simplest and most immediate way ahead was to prepare and test a group of specimens; fig. 10 shows that the detrimental effect is small for the thick joint variant, and appreciable mainly at low stress levels.

Fig. 10 also shows the results of the specimens that were subjected, after to the TSA treatment, also to the CX process. In this case, a 4% nominal expansion was performed, and a light interference fit was used for inserting the fasteners, that means 0-30 μm interference. In the short life range, the CX results show an increase in life of a factor about 2, while at low amplitude, particularly approaching the endurance limit, the enhancement factor increases; this behavior is in line with expectations. In the literature, a high number of similar results are available, that show how the level of improvement is dependent on the configuration: each joint has a specific stress distribution, directly depending on the geometry (load transfer, secondary bending, etc.), and normally a high stress concentration.

A first set of Laser Shock Peened specimens (LSP) was assembled and tested. The LSP process was applied in the areas of holes 1 and 2, namely the critical location and its neighbor hole (see fig 1). These areas did not require any special treatment for the drilling of the final hole, while it was considered appropriate to apply a CX treatment to the two remaining holes (holes 3 and 4), in order to avoid some unexpected failure, particularly in hole 4. The split sleeve Cold eXpansion was applied following the same procedure of the CX specimens; in conclusion, each hole in the LSP joints received a fatigue enhancement treatment.

Fig. 11 shows that "thick" TSA+LSP and TSA+CX groups of results are almost indistinguishable, with a slightly better behavior of the LSP treatment at low stress levels. In this group two cases of "double failure" (i.e. in hole 1, the expected location, and in hole 4, the opposite location) were observed, and are highlighted by solid symbols.

4.2.2 Thin specimens

The testing of thin specimens is still in progress, because the optimization of the LSP process parameters has not yet been concluded and so only the results of the other groups of thin joints will be commented. The results will be presented, starting as before from the "basic material" group, which was tested to provide a reference. Fig. 12 shows the results. The scatter is relatively low, with the exception of two cases, evidenced by a filled symbol, which have been excluded from the best-fit analysis. Such points refer to specimens where the failure did not initiate in correspondence of the hole net section, but slightly outside. This is typically observed in riveted joints when the squeeze force is very high, and so the shank material fills the hole very well: initiation may then be promoted by fretting under the rivet head. Apparently, a similar failure process occurred also in these two specimens.

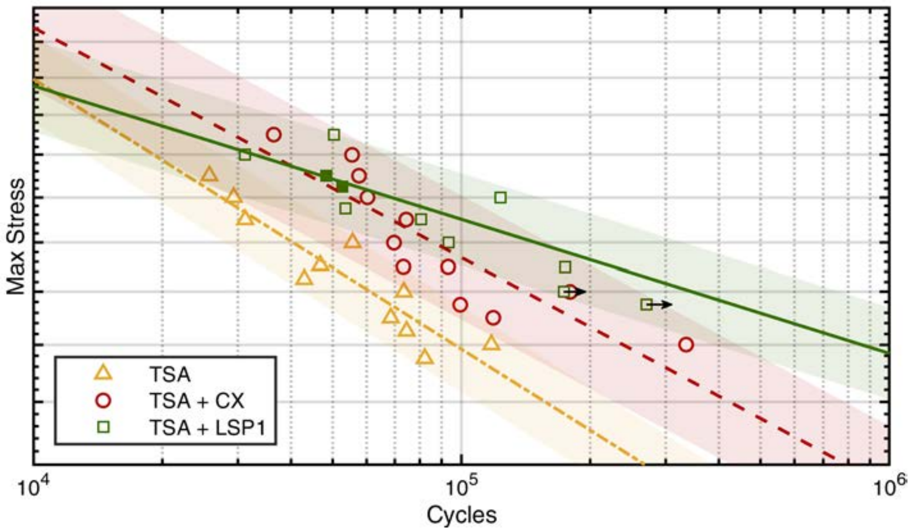

Fig. 11 – Whöler curves for thick variant: advanced treatments

This event may be connected with an excessive force inadvertently applied during fastener installation (it occurred only in such 2 cases).

Coming to the presentation of the TSA results, they are also shown in fig. 12. The scatter in the TSA results is a bit higher than in the case of the basic material, and also a small, but clear, reduction in fatigue performance can be appreciated in the graph. The TSA results are slightly translated down, and the best-fit lines are almost parallel.

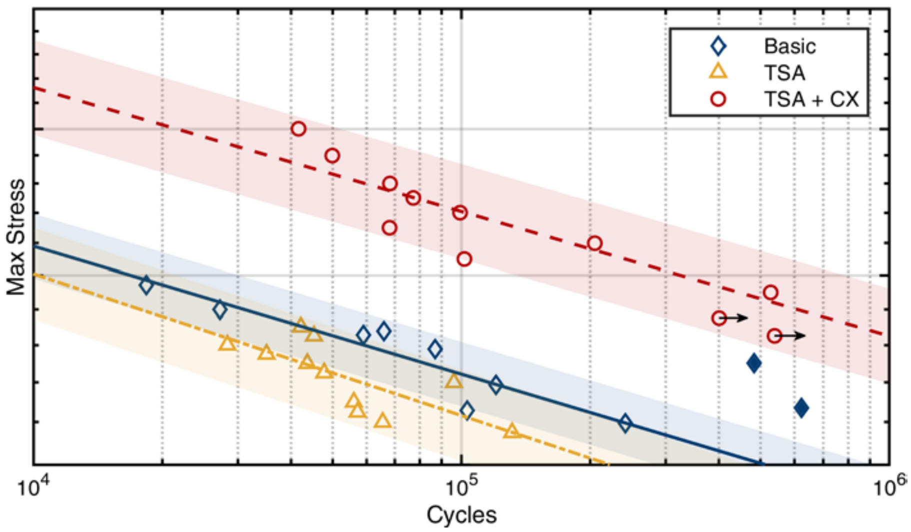

Fig. 12 – Whöler curves for thin variant: basic treatments

On the contrary, the results from the TSA+CX specimens show an improvement in fatigue performance with respect to the TSA results which is relevant: the increase in life can be quantified, at equal stress level, in about 15 times.

4.3 Crack surfaces

After the end of the fatigue test, each specimen was checked and its fracture surfaces examined, in order to detect any possible anomaly. The examination of the fracture surfaces is easier for the thick specimens, because in those cases the area associated with fatigue propagation was much higher. The strong influence of the microstructural features of the extrusion makes the surface appearance quite particular: fig. 13 shows a few examples relevant to thick specimens. The surfaces have a wavy appearance, quite particular with respect to what can be observed normally in plates and sheets; such a character is not reduced by the introduction of residual stresses, but maybe made even more evident.

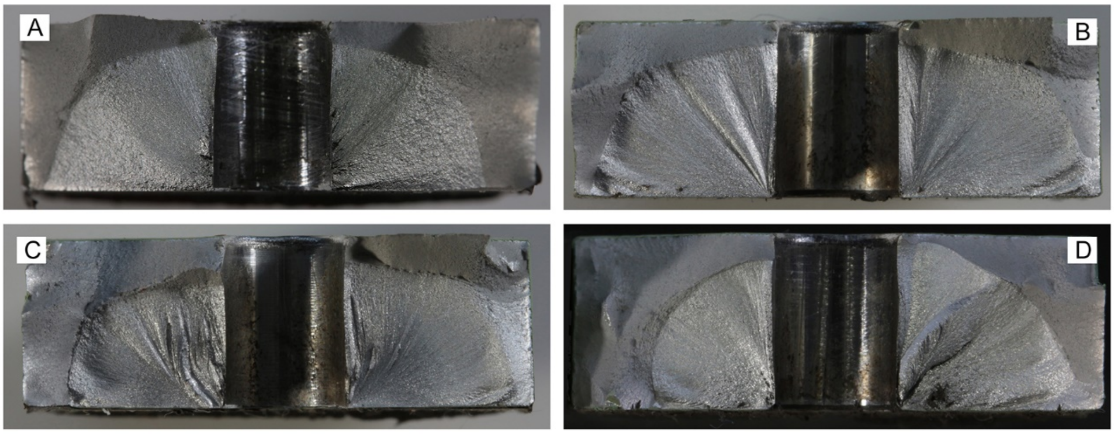

Fig. 13 – Examples of different types of fracture surfaces (A: Basic material; B: TSA; C: TSA + CX; D: TSA + LSP).

5. Conclusions

The experimental activity described in this paper has allowed the evaluation of some processes typically applied in aircraft structures to improve their fatigue resistance. The discussion of the results can be summarized by the following conclusions:

a. the two joint configurations evaluated (thin and thick) are substantially different, not simply two similar specimens scaled in dimension. The thick variant is more fatigue critical, because there is more SB while the fastener diameter is the same.

b. TSA treatment has a negative effect on the fatigue performance, as expected and in accordance with similar results from other anodization treatments. It has a different influence on the thin and thick variants (more sensible in the first and less in the second), which can be explained with the higher stress concentration associated with the thick variant.

Indeed, the TSA treatment can be included into the surface effects, like for instance the finish. Such surface effects have a larger influence in an S-N curve at lower stress levels, when lives are longer; at high stress levels, initiation takes place irrespectively of the surface finish, because it is dominated by the stress concentration. In a similar way, the surface effect is higher for lower Kt's values and so, between the two specimen configurations, the thin coupon is expected to be more sensitive to the effect (the secondary bending makes the thick configuration affected by a higher stress concentration, testified by a reduction in maximum cyclic stress for equal life).

c. the traditional split sleeve CX process is capable of improving significantly the fatigue life (the more in thin components, where the SB is lower).

d. the innovative LSP process is a very promising and powerful tool, at least comparable with the benefits that can be obtained from the CX process, in the thick joints. Work is still in progress for optimizing the various process parameters in order to obtain a residual stress field, with given characteristics of distribution and intensity, also in thin components.

6. Contact Author Email Address

mailto: daniele.fanteria@unipi.it

7. Copyright Statement

References

[1] Schijve J., *Fatigue of Structures and materials,* Kluwer Academic Publishers, ISBN 0-7923-7013-9 (2001). 2nd edition, Springer, ISBN 978-1-4020-6807-2, (2009)

[2] Coombe, T., Urzi, R. B. Critically loaded hole technology pilot collaborative test programme, Advisory Group for Aerospace Research & Development, AGARD Report 678, Nov. 1980, ISBN 92-835-1375-4.

[3] van der Linden, H.H., Urzi, R. B. Fatigue rated fastener systems, Advisory Group for Aerospace Research & Development, AGARD Report 721, Nov. 1985, ISBN 92-835-1512-9.

[4] Jarfall, L. Shear Loaded Fastener Installations. SAAB-SCANIA report KHR-3360, Linkoping, Sweden, 1983. Also: Int. J. of Vehicle Design, vol. 7, 1986, pp. 337-380.

[5] Segerfrojd, G., Wang, G.S., Palmberg, B. and Blom, A.F. Fatigue behaviour of mechanical joints: critical experiments and statistical analysis, in Fatigue in new and ageing aircraft (R. Cook and P. Poole eds.) Proc. 19th ICAF Symposium, EMAS publ., (1997), pp. 575-598.

[6] Anon. Derivation of endurance curves from fatigue data, including run-outs. Engineering Sciences Data Unit 97024.